JOURNAL OF CATALYSIS 51, 326–337 (1978)

Structure, Formation, and Stability of Paracrystalline Ammonia Catalysts[1]

H. LUDWICZEK AND A. PREISINGER

Institut für Mineralogie und Kristallographie der Universität Wien, Vienna, Austria

AND

A. FISCHER, R. HOSEMANN, A. SCHÖNFELD, AND W. VOGEL

Fritz-Haber-Institut der Max-Planck-Gesellschaft, Teilinstitut für Strukturforschung, Berlin-Dahlem, Germany

Received February 14, 1977; revised October 24, 1977

X-ray diffraction and high-precision line profile analysis in combination with Mössbauer spectroscopy and secondary ion mass spectroscopy (SIMS) support the result that Al_2O_3-promoted ammonia catalysts consist of paracrystallites caused by endotactic "Al_2FeO_4" groups. In samples of magnetite with a content of $<3\%$ Al_2O_3 reduced at 350–500°C, there are mostly individual "Al_2FeO_4" groups endotactically built into the α-Fe lattice to form paracrystallites ("α-Fe"). The high stability of the large surface of the "α-Fe" is a consequence of the paracrystallinity and is one important and necessary condition for an efficiently working catalyst, which unfortunately was not taken into consideration adequately in the past. Generally, paracrystalline "α-Fe" can be formed by groups of X_2FeO_4 with trivalent cations X such as Al, Sc, Cr, etc. The formation mechanism of "α-Fe" such as these at <600°C goes directly by the reduction of spinel. In the case of divalent cations such as Mg, where under such conditions no paracrystallinity is observed, the formation of "α-Fe" goes over the intermediate magnesia wüstite phase, (Fe, Mg)O, and has no thermostable large inner surface. It remains an open question how far the liquid-like distortions on the surfaces of the microparacrystals influence the catalytical activity.

I. INTRODUCTION

Since the beginning of this century when Haber and Bosch developed a practical ammonia synthesis, ammonia catalysts have been of industrial importance. These catalysts consist of metallic iron particles (mean diameter, 350 Å) with metal oxide promotors, where the oxides are oxides of mono-, di-, or trivalent metals or combinations thereof. They are prepared from quenched spinel mixed crystals (magnetite + $\sim 2\%$ metal oxides) by reduction in a stream of H_2 or H_2–N_2 at 400–500°C.

For this type of catalyst, summarized in articles by Frankenburg (*1*) and Nielsen (*2*), a model is given in which the promoting oxides partially covered the surfaces of the α-Fe crystallites. In 1966 Hosemann *et al.*, based on their studies of Al_2O_3-promoted α-Fe (*3*), suggested another model in which paracrystalline distortions exhibited by this catalyst are caused by "Al_2FeO_4" groups endotactically built into the α-Fe lattice.

Pernicone *et al.* (*4*) confirmed the paracrystallinity for Al_2O_3-promoted α-Fe catalysts reduced at 500°C and with DTA measurements indirectly showed the presence of "Al_2FeO_4" in the α-Fe paracrystallites.

[1] Dedicated to Professor Dr. Werner Köster on the occasion of his eightieth birthday.

0021-9517/78/0513-0326$02.00/0

Further, these authors found that two other trivalent promoting oxides, Sc_2O_3 and Cr_2O_3, also caused paracrystalline distortions. However, catalysts prepared by reduction in a stream of H_2 at 500°C but promoted with divalent oxides such as MgO and MnO, exhibited no paracrystallinity.

In addition, Fagherazzi *et al.* (*5*) determined that the lattice constants of the catalysts differed by less than 0.02% from those of pure α-Fe, which is in agreement with (*2*) and (*3*), and that the magnetic hyperfine splitting in the Mössbauer spectra was identical with that in pure α-Fe. Contrary to the results in (*3*), they conclude that iron aluminate forms clusters (<25 Å, on the average) inside the α-iron.

Topsøe *et al.* (*6*) also showed that the hyperfine splitting in the Mössbauer spectra of a 3% Al_2O_3-promoted α-Fe was essentially the same as for pure α-Fe. Nevertheless, they concluded that Al_2O_3 clusters 30 Å in diameter must be present in the fully reduced α-Fe crystallites.

Using secondary ion mass spectrometry (SIMS), Buhl and Preisinger (*7*) confirmed the presence of "Al_2FeO_4" groups, but the absence of Al_2O_3 clusters was noted in the catalysts of Hosemann, *et al.* (*3*).

The goal of this study was to obtain an understanding of the structure, mechanism of formation, and stability of paracrystalline ammonia catalysts. For this first step catalysts with only one metal oxide as promotor were investigated.

II. EXPERIMENTAL

1. Sample preparation. Samples of magnetite with 3 wt% of MgO and with 1, 2, 3, and 5 wt% of Al_2O_3, respectively, were melted in an electric arc furnace at 3000°C and then quenched to room temperature so that a homogeneous distribution of oxide in the Fe_3O_4 matrix would be obtained [2]

The starting materials were ground in an agate mortar, and then the samples were reduced at different reduction conditions and temperatures. For the reduction of the spinels at ≥400°C, H_2 from Linde AG (<1 vol ppm of O_2, H_2O) was used.[3] For the reduction of the spinels <400°C, H_2 purified with CrO_3–silica gel was used.[4] All reduced samples were cooled to room temperature in a stream of N_2.

2. X-ray diffraction and line profile analysis. Samples for diffraction studies were prepared in a N_2 atmosphere, and the finely powdered specimens were imbedded with an UHU-acetone solution between Hostaphan foils. The diffraction diagrams were taken on Agfa OSRAY T4 film at 20°C using a high-resolution AEG-Guinier camera according to the method of Hofmann and Jagodzinski (*8*) with Cr$K\alpha$1 and Co$K\alpha$1 radiation as well as Mo$K\alpha$2 for the reflections with higher indices. The observed line profiles were recorded with a Joyce–Loebel double-beam photometer. The standard consisted of Fe powder annealed at 800°C and prepared with the same thickness as the samples. The resolution for Cr and Co radiation in this arrangement is about 1700 Å. Since the α-Fe crystallites of the standard are relatively large, the line profile of an α-Fe reflection is very sharp with a half-width smaller than that of the collimator. Therefore, the recorded line profile is that of the collimator: Lorentzian square. The observed particle sizes in the promoted α-Fe are much smaller than 1700 Å; thus in many cases the collimator does not strongly affect their line profiles. According to the theory of paracrystals, the line profiles are given by the convolution product of the paracrystalline lattice factor and the shape factor. The former factor always gives Lorentzian shapes. The

[2] We are indebted to Dr. H. Friz, Director, BASF AG, Ludwigshaven, for the preparation of both sets of samples.

[3] We are grateful to Dr. K. D. Otten, TU Berlin, for the reduction of these samples.

[4] We are grateful to Prof. Dr. H. L. Krauss, FU Berlin, for the reduction of these two samples.

latter depends on the particle size distribution, and in our case we have the Lorentzian-square type. Therefore the higher-ordered reflections from the promoted α-Fe have a Lorentzian shape, and those of the lower-ordered reflections have a shape between Lorentzian and Lorentzian square.

The paracrystalline distortions of a family of lattice planes *hkl* are defined by

$$g_{hkl} = (\overline{d_{hkl}^2}/\bar{d}_{hkl}^2 - 1)^{\frac{1}{2}} \qquad (1)$$

where $\bar{d}_{hkl}$ is the average of the interplanar spacing.

For the unambiguous determination of the paracrystallinity g_{hkl}, three orders of a reflection from a family of lattice planes must be available by the evaluation of the integral widths. Since in our case the reflection (411) coincides with (330), the value of g_{110} was determined from the integral widths of the reflections (110), (220), and (440). Also, a line profile analysis according to an expanded Fourier method from Warren (*10*) was done. This method has the advantage that only two orders of a reflection are necessary to distinguish between paracrystalline distortions and mechanical microstresses [Vogel *et al.* (*11*)].

3. Mössbauer spectroscopy. The γ-ray resonance absorption spectra of ^{57}Fe were made with a 1052-channel analyzer in conjunction with a Doppler velocity generator operated at constant acceleration and symmetric wave form. The source was ^{57}Co diffused into a palladium foil. The detector was a proportional counter filled with Xe and CO_2. The counting rates of the spectra varied between 0.32 and 0.37 $\times$ 10^6 counts per channel. The absorber density was 10 mg of natural Fe/cm^2. The absorber consisted of the powdered substance sandwiched between Mylar foils with a 2.0-cm diameter. Separate mirror-symmetric spectra (2 $\times$ 512 channels) for part of the samples were made for least-squares fits which were then averaged. Refinement was done assuming a Lorentzian form for the absorption lines. The error for χ^2 per channel was 1.0–1.5 units.[5]

4. Secondary ion mass spectrometry (SIMS). The experimental investigations were made with a Balzers secondary ion mass spectrometer on a promoted "α-Fe" with 3 wt% of Al_2O_3 which had been reduced at 400°C from M-2.2Al (*7*) and on an M-3Al sample reduced at 600°C in a stream of H_2.[6] The spectra were maintained at a primary argon energy of 500–1000 eV and a current density on the sample of 10^{-7}–10^{-8} A cm^{-2}.

III. RESULTS

1. Unreduced Starting Materials. The quantitative phase compositions, lattice constants, and particle sizes of the unreduced samples M-1Al, M-2A1, M-3Al, and M-5Al (magnetite + n wt% of Al_2O_3) are given in Table 1. The spinel, $Fe_{3-x}Al_xO_4$, homogenized at 3000°C and quenched to room temperature, showed an exsolution into wüstite ($Fe_{1-x}O$) and/or hematite (α-Fe_2O_3). With increasing promotor content, decreasing amounts of wüstite and slightly increasing amounts of hematite were observed.

Since the lattice constants in the magnetite (Fe_3O_4)–hercynite ($FeAl_2O_4$) system follow Vegard's linear law (*12*), with the aid of Fig. 1 the chemical compositions of the $Fe_{3-x}Al_xO_4$ mixed crystals can be determined. These are given in Table 1.

Spinels with $x \leq 0.137$ prepared in this way show no exsolution into magnetite and hercynite. Their crystal sizes are larger than 1500 Å. In spinels with more than 3% Al_2O_3, exsolution occurs as already pointed out by Hosemann, *et al.* (*3*).

As can be seen from Fig. 2, sample M-5Al shows an exsolution into three spinel components: Component I (32 wt%)

[5] We thank Professor St. Hafner and Dr. Amthauer, University of Marburg, and Dr. Stein, TU-Vienna, for the Mössbauer measurements.

[6] We thank Dr. R. Buhl, Balzers AG, for the measurements.

TABLE 1

Compositions of the Unreduced Samples

Phase		M-1Al	M-2Al	M-3Al	M-5Al		
					I	II	III
Spinel	wt%	89	89	93	32	60	3
($Fe_{3-x}Al_xO_4$)	a (Å)	8.390 (1)	8.385 (1)	8.379 (1)	8.39 (1)	8.354 (1)	8.31 (1)
	$\bar{L}_{111}$(Å)	>1500	>1500	>1500		>1500	
		$x = 0.053$	$x = 0.092$	$x = 0.137$	$x = 0.05$	$x = 0.328$	$x = 0.66$
Wüstite	wt%	4 7	6 4	3 2		—	
($Fe_{1-x}O$)	a (Å)	4.327 (1) 4.293 (1)	4.325 (1) 4.288 (1)	4.321 (1) 4.286 (1)		—	
	$\bar{L}_{200}$(Å)	n.d.[a] n.d.	500 n.d.	n.d. n.d.		—	
Hematite	wt%	—	1	2		5	
(α-Fe_2O_3)	a (Å)	—	5.025 (1)	5.025 (1)		5.025 (1)	
	c (Å)	—	13.735 (2)	13.735 (2)		13.735 (2)	

[a] n.d. = not determined.

consists of microcrystals with the chemical composition $x = 0.05 \pm 0.05$; component II, the main part (60 wt%), with $x = 0.328 \pm 0.001$ and a crystal size of >1500 Å with some individuals >1 μm; component III (3 wt%) with $x = 0.66 \pm 0.06$.

The ferrous oxide phases of samples M-1Al, M-2Al, and M-3Al exhibit a splitting of the lattice constants. While the larger lattice constants correspond to a relatively stoichiometric FeO content, the smaller ones are more a result of non-stoichiometric wüstite ($Fe_{1-x}O$) with Fe vacancies and the resulting lower Al and/or Fe(III) concentrations.

2. *Reduced Samples*

The starting materials M-1Al, M-2Al, M-3Al, and M-5Al (Table 1) were reduced with H_2 at 400°C for 144 hr. The amounts of reaction products (weight percent), the lattice constants (a, in angstroms), the particle sizes ($\bar{L}_{110}$, in angstroms), and the paracrystallinity (g_{110}, as a percentage) as determined by X-ray analysis are given in Table 2. Moreover, no phases other than promoted iron and spinel were found. The spinels are composed of $Fe_{3-x}Al_xO_4$, where x is given from the lattice constants in combination with Fig. 1. The promoted iron, called "α-Fe," has essentially the same lattice constant as pure α-Fe but shows paracrystallinity. The values for the weight percent of Al_2O_3 in the phase "α-Fe" were calculated from the difference between the Al_2O_3 concentration in the starting materials and the spinel in the reduced samples.

Under these reduction conditions, according to Akimov (*13*), the reduction rate

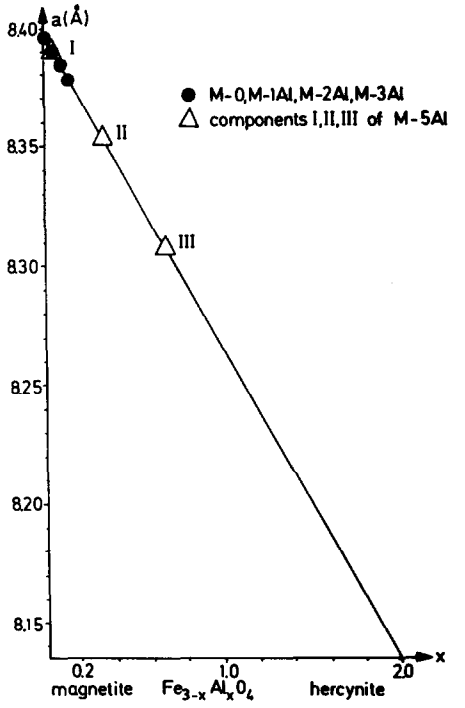

FIG. 1. Lattice constants of $Fe_{3-x}Al_xO_4$ in the system magnetite (Fe_3O_4; $a = 8.397$ Å, $x = 0$)–hercynite ($FeAl_2O_4$; $a = 8.135$ Å, $x = 2$). The full line follows Vegard's linear law. The magnetite of M-5Al consists of three components (I, II, and III).

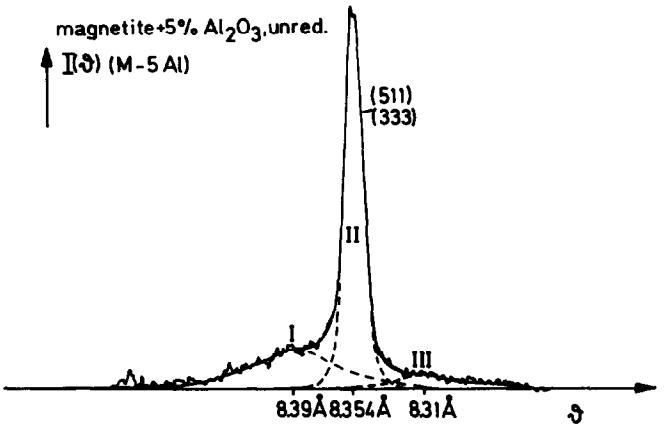

FIG. 2. Line profile of the (511) + (333) reflections of the three spinel components of M-5Al.

becomes somewhat slower with increasing amounts of Al_2O_3 in the starting material, so that the spinel is fully reduced only for samples with $<2\%$ Al_2O_3 (M-2Al). The higher reduction rate for M-5Al is due to the component I which reduced much faster than component II. Figure 3 shows the results of the reduction process of M-3Al and M-5Al in the (311) reflections. The linewidths indicate that the size of component III is much smaller than that of component II. Component I has been completely reduced.

To check the phase compositions, Mössbauer spectra were made for the partially reduced M-3Al (Table 2) and compared with pure α-Fe and Fe_3O_4 (Table 3). The partially reduced M-3Al shows only two phases: "α-Fe" and spinel. The "α-Fe" shows no significant change regarding the position of the magnetite hyperfine splitting as compared with pure α-Fe, as already

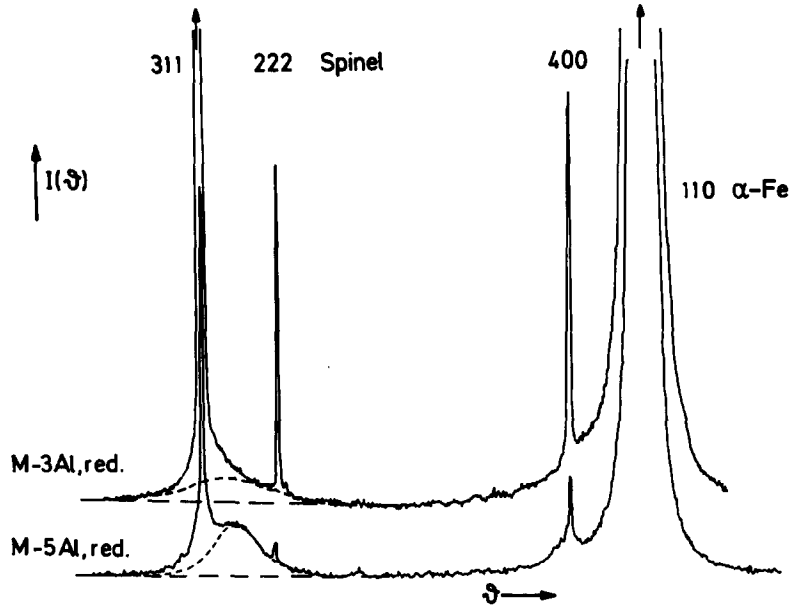

FIG. 3. Comparison of the (311) reflection of the two spinel components (II and III) of partially reduced M-3Al and M-5Al.

shown by Fagherazzi *et al.* (*5*) and Topsøe *et al.* (*6*) for fully reduced samples. Only a slight line broadening was discernible (Table 3). The spinel phase in this sample shows a decrease in the magnetic hyperfine splitting. The relationship of the areas of peaks 1 to 6 and A_1 to A_6 plus B_1 to B_6 gives a ratio "α-Fe":spinel $\simeq 3$, which is in agreement with X-ray results.

It can be concluded from these analytical results using X-rays and the Mössbauer effect that the reduction process at 400°C goes directly, without any intermediate phases, from the spinel phase to the paracrystalline "α-Fe." In the unreduced spinels, Al is enriched. Al_2O_3-promoted samples reduced below 600°C all show a reaction mechanism direct from spinel to "α-Fe."

Since no paracrystallinity occurs in MgO-promoted α-Fe [Perricone *et al.* (*4*)], the reaction mechanism for a magnetite doped with 3% MgO was studied using X-ray and Mössbauer effect measurements. The incomplete reduction of M-3Mg at 400°C produces, besides wüstite and α-Fe, the unchanged spinel [$Fe_{3-x}Mg_xO_4$; $x = 0.170$; $a = 8.394(1)$]. In the wüstite phase an enrichment in Mg to up to 60% of the cation positions is observed. Contrary results for M-3Al, by the reduction of M-3Mg at 400°C and higher (500°C), an intermediate wüstite phase forms, and from this α-Fe develops.

As can be seen from Table 2, under the same reduction conditions the paracrystallinity (g_{110}) of "α-Fe" increases with increasing percentages Al_2O_3, while the mean particle size ($\bar{L}_{110}$) decreases.

M-3Al was also reduced at 350°C with H_2 for 24 hr. Besides an unreduced spinel [$a = 8.375(1)$ Å], promoted iron ["α-Fe"; $a = 2.866(1)$ Å, $\bar{L}_{110} = 330$ Å, $g_{110} = 1.30\%$, and ~3.4 wt% of Al_2O_3] resulted.

To assure the absence of any significant microstresses, above 450°C a recovery of microstresses in α-Fe is known to take place within a few seconds (*14*), the reduced samples were heated to 500°C for 20 sec

TABLE 2

Reduction in H_2 of the Starting Materials M-1Al, M-2Al, M-3Al, and M-5Al at 400°C for 144 hr

Phase		Starting materials											
		M-1Al	M-2Al			M-3Al			M-5Al				
			II	III		II	III		I	II	III		
Spinel ($Fe_{3-x}Al_xO_4$)	wt%	0	10	~1		20	~2		0	10	10		
	a (Å)	—	8.375 (1)	~8.25		8.370 (1)	~8.23		—	8.362 (1)	8.21 (1)		
			$x = 0.185$	$x \approx 1.12$		$x = 0.200$	$x \approx 1.28$			$x = 0.270$	$x = 1.42$		
Promoted iron ("α-Fe")	wt%	100	89			78			80				
	a (Å)	2.866 (1)	2.866 (1)			2.866 (1)			2.866 (1)				
	$\bar{L}_{110}$ (Å)	500	460			340			275				
	g_{110} (%)	0.81	1.08			1.13			1.10				
	wt% of Al_2O_3	~1.35	~2.3			~2.9			~2.6				

TABLE 3

Hyperfine Interactions from the Mössbauer Spectra of Partially Reduced M-3Al (Table 2), α-Fe, and Fe_3O_4 at 298 K

Sample	Phase			
	"α-Fe"[a]			Spinel[b]
	Δ	δ	Γ̄	Δ
M-3Al (reduced at 400°C)	10.651 (2)	−0.184 (2)	0.345 (5)	14.82 (3)
α-Fe	10.633 (2)	−0.172 (2)	0.230 (5)	
Fe_3O_4				15.32 (5)

[a] "α-Fe": Δ, magnetic hyperfine splitting (6 − 1) [mm/sec]; δ, chemical isomer shift (6 + 5 + 2 + 1)/4 [mm/sec]; Γ̄, linewidth at half-height $(B_1 + B_6)/4$ (mm/sec].

[b] Spinel: Δ, magnetic hyperfine splitting $(A_6 + B_6 - A_1 - B_1)$[mm/sec].

in He. Their g values showed essentially no change.

The change of the paracrystallinity under different conditions is shown in Fig. 4. Sample M-2.2Al [Hoscmann *et al.* (*3*)] fully reduced at 400°C ("α-Fe"; a = 2.866 Å, g_{110} = 1.04%, $\bar{L}_{110}$ = 250 Å) was additionally reduced in H_2 for 20 hr at 800°C and for 10 hr at 950°C. At 800°C only "α-Fe" with a = 2.866 Å, $\bar{L}_{110}$ = 560 Å, and g_{110} = 0.60% was observed by X-ray. At 950°C besides α-Fe (a = 2.866 Å, $g_{hkl} \simeq 0$%), β-Al_2O_3 was observed. According to Faghcrazzi *et al.* (*5*) a sample M-1.3Al, fully reduced at 500°C ("α-Fe"; a = 2.866 Å, $\bar{L}_{110}$ = 330 Å, g_{110} = 1.00%), was subdivided into three parts which were additionally heated in an inert atmosphere at 800, 900, and 950°C for 20 hr. At 800 and 900°C only "α-Fe" with decreasing g values (g_{110} = 0.74 and 0.49%, respectively) and increasing $\bar{L}$ values ($\bar{L}_{110}$ = 360 and 590 Å, respectively) was observed. At 950°C, in addition to α-Fe with $g_{hkl} \simeq 0$%, hercynite ($FeAl_2O_4$) was observed.

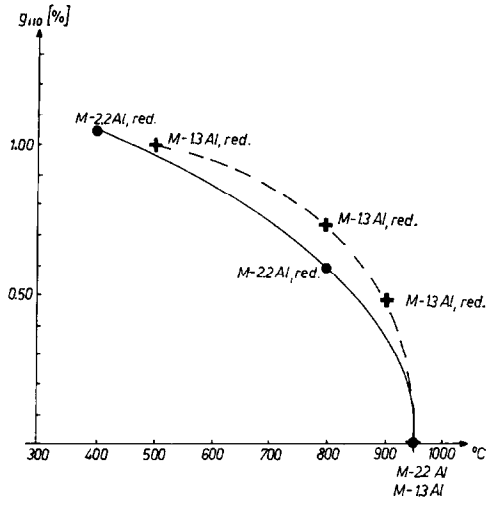

FIG. 4. Paracrystallinity, g_{110}, as a function of temperature treatments of reduced samples under H_2(——) (*3*) and under inert gas (– – – –) (*5*) conditions.

For the sample M-2.2Al fully reduced at 400°C to "α-Fe" (*3*) secondary ion mass spectra (SIMS) were taken by Buhl and Preisinger (*7*). The polyatomic ions sputtered from the "α-Fe" included the following: $(AlO)^+$, $(AlO)^-$, $(AlO_2)^-$, $(FeO)^+$, $(FeO)^-$, $(FeAl)^+$, $(FeO_2)^-$, $(AlOFe)^+$, $(FeO_3)^-$, $(Fe_2)^+$, $(AlO_2Fe)^+$, $(Fe_2Al)^+$, $(FeO_2Fe)^+$, $(OFe_2O)^-$, $(AlO_2FeO_2)^-$, $(AlO_2FeO_2Al)^+$, $(AlO_2FeO_2Al)^-$, $(AlO_2FeO_2Fe)^+$, and $(FeO_2FeO_2FeO_2Fe)^-$. Polyatomic ions of the forms $(Al_2)^+$, $(Al_2O)^+$, $(AlO_3)^-$, $(AlO_2Al)^+$, $(OAl_2O)^-$, and $(Al_2Fe)^+$ were not observed. In Preisinger and Buhl's work (*7*) it was concluded from the masses of the observed and unobserved polyatomic ions that in this "α-Fe" no Al_2O_3 clusters can be present but that Al_2FeO_4 groups must be built into the α-Fe lattice.

An additionally fully reduced M-3Al, in H_2 at 600°C to "α-Fe", showed among other polyatomic ions a decrease in $(FeAl)^+$ of about half and observations of $(Al_2O)^+$, $(AlO_3)^-$, $(Al_2O_2)^\pm$, and $(Al_2O_3)^-$.

IV. DISCUSSION

1. *Structure of Paracrystalline Iron, "α-Fe"*

As already published (*3*, *7*), a very reasonable model for the Al_2O_3-promoted ammonia catalysts, "α-Fe", is one containing polyatomic groups composed of Al_2FeO_4 each of which endotactically replaces a group of seven Fe atoms in the α-Fe particles. These endotactic groups (AlO_2FeO_2-Al) lie with their Al–Fe–Al axis parallel to a [100] axis of the cubic α-Fe lattice so that each Al is coordinated by two O and six metallic Fe atoms. The Fe in the middle of this group is tetrahedrally coordinated by 4 O (Fe–O distance, ~2.1 Å). Each of the O is coordinated by one Al, one Fe, and six metallic Fe atoms. These endotactic groups are statistically distributed in the "α-Fe." Under reducing conditions, groups lying on the surface of "α-Fe" are reduced to aluminum oxides without iron (Fig. 5).[7]

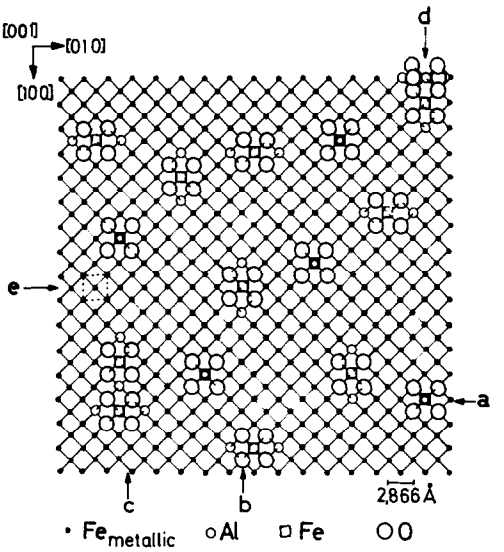

FIG. 5. Projection of a part of "α-Fe" parallel to [001] ideally drawn without paracrystalline distortions. In reality the surface planes are uneven. a, endotactic Al_2FeO_4 groups with the Al–Fe–Al axis parallel to [001]; b, endotactic Al_2FeO_4 groups with the Al–Fe–Al axis parallel to [010]; c, cluster of two Al_2FeO_4 groups; d, aluminum oxide groups on the surface without Fe ions.

Since the Al_2FeO_4 groups do not fit exactly in the α-Fe lattice, they produce paracrystalline distortions. If in "α-Fe" γ is the numerical concentration of independent endotactic groups and 100 $(\overline{dR/R})$ is the percentage difference, in a crystallographic direction, between the size of the group and the Fe atoms it replaces, it then follows, in a simplified one-dimensional treatment (*16*), that for this direction

$$g_{hkl} = \left(\frac{\overline{dR}}{R}\right)[\gamma(1-\gamma)]^{\frac{1}{2}}. \qquad (2)$$

If the concentration of $\gamma \ll 1$ (in the treated samples it is about 1%; that is, $\gamma \simeq 0.01$), then

$$g_{hkl}\Big/\left(\frac{\overline{dR}}{R}\right) \simeq \gamma^{\frac{1}{2}}. \qquad (3)$$

In the [110] direction $(\overline{dR/R})$ is ~0.09. In Fig. 6 $[g_{110}/(\overline{dR/R})]^2$ is plotted against γ_{max}, the concentration of the Al_2FeO_4 groups calculated from the weight percent of Al_2O_3 in "α-Fe." For line *s* in Fig. 6 the number of independent endotactic groups equals the number of Al_2FeO_4 groups ($\gamma = \gamma_{max}$). If the number of Al_2FeO_4 groups is greater than the number of independent endotactic groups ($\gamma_{max} > \gamma$), then part of the Al_2FeO_4 groups have formed clusters of $(Al_2FeO_4)_n$. Figure 5, letter c, shows a cluster of two Al_2FeO_4 groups ($n = 2$). As can be seen from Fig. 6, if the promoted catalyst is reduced at ≤400°C,

[7] Pernicone *et al.* (*4*) estimate, by CO and N_2 chemisorption, according to Emmett's method, 90% free iron surface for samples with 1% Al_2O_3 and 70% free iron surface for samples with 3% Al_2O_3.

within experimental error the majority of the Al_2FeO_4 groups occur as isolated groups.

The number of Al_2FeO_4 groups within a cluster cannot be too large if paracrystalline distortions exist. Their limit in a particular direction is given by $n\Delta R < (d_{hkl}/2)$, where $n\Delta R$ is the difference between the atomic distances of the host lattice and that of the cluster, and d_{hkl} is the interplanar spacing; otherwise the clusters are too large for endotactic groups and will precipitate inside the α-Fe lattice. No paracrystallinity can be produced by such independent precipitates. In the [110] direction n of these clusters must be less than 3, then ΔR is $\sim$0.3 Å, d_{110} is $\sim$2.1 Å, and therefore the diameter of a cluster must be less than $\sim$6 Å.

These results are in best agreement with the above-mentioned Mössbauer measurements. The hyperfine splitting Δ is the same in "α-Fe" as in α-Fe except for a slight line broadening. This means that the crystal chemical properties of "α-Fe," such as lattice constant (*3*), Curie point (*5*), and the density of states of electrons, are not changed relative to pure α-Fe.[8] Contrary to this is the case for Fe–Al alloys with low Al concentrations (*17*, *18*).

Because of the relatively few endotactic Fe atoms, a separate Mössbauer signal will be comparatively very weak. Because of the unevenness of the lattice planes, the environment of an endotactic group depends on its location within the paracrystal. The environment also depends on whether the group is isolated or in a cluster. These different environments cause slight shifts in the signals which act to broaden the weak peak. Thus, instead of a separate sharp peak for the Fe atoms in the endotactic groups, only a slight increase in the background between 0 and -1 [mm/sec] may be observed.

[8] A more distinct effect of the endotactic Al_2FeO_4 groups in "α-Fe" is to be expected, if one starts with mixed spinels of Al_2 $^{57}FeO_4$ with $^{56}Fe_3O_4$ (S. Prakash, in preparation).

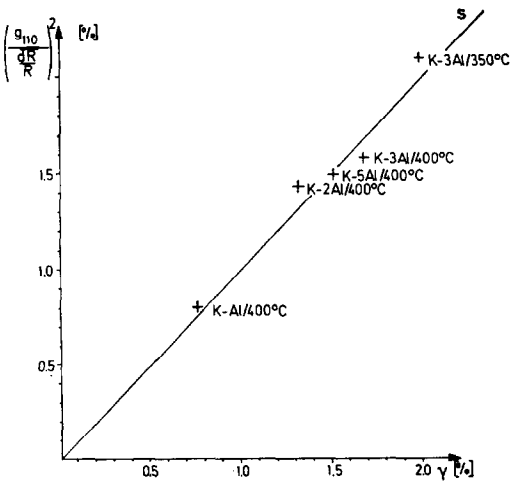

FIG. 6. M-nAl samples reduced in H_2 at $\leq$400°C plotted in the diagram as percentage of endotactic groups $[g/(\overline{dR/R})]^2 = \gamma$ against percentage of Al_2FeO_4 groups $[\gamma_{max}]$.

2. Formation of Paracrystalline Iron, "α-Fe"

By the reduction of pure magnetite, α-Fe is formed directly below 570°C but through the intermediate wüstite phase above that temperature (*19*). As shown by X-ray investigations and Mössbauer measurements, magnetite-rich mixed crystals of the type $Fe_{3-x}Al_xO_4$ are converted directly to "α-Fe" at temperatures >350°C and <600°C, while $Fe_{3-x}Mg_xO_4$ mixed crystals (i.e., $x = 0.170$) are converted to α-Fe through an intermediate wüstite (Fe_{1-y}-Mg_yO) phase in the temperature range 400–500°C. The divalent Mg ions thereby enriched in the wüstite stabilize it below 570°C, and the reduction to α-Fe follows from the magnesia wüstite. Since Fe and Mg are octahedrally surrounded by six O in this phase, the formation of endotactic groups with four coordinate Fe does not take place. In the case of the trivalent cations (X = Al, Sc, Cr, etc.) built into spinel, the reduction process allows the formation of endotactic "X_2FeO_4" groups. The numerical concentration (γ) of the endotactic groups in "α-Fe" depends on the temperature and the reducing conditions. Together γ and $\overline{dR/R}$, the latter

being the measure of the average deviation of the size of the endotactic group from the equivalent size of the host lattice, determine the relative statistical variation g_{hkl} of the interplanar spacing d_{hkl}, the average unevenness of the lattice planes. According to the fundamental properties of paracrystals (*16*), the surface unevenness of the lattice planes is limited by a material constant of the host lattice,

$$\alpha^*_{hkl} = g_{hkl}(N_{max})^{\frac{1}{2}}, \qquad (4)$$

where $N_{max} = \bar{L}_{hkl}/d_{hkl}$, the number of lattice planes in the (hkl) family within the paracrystal. Since the observed $\bar{L}_{hkl}$ values, which depend on the material constant of the host lattice, will also be influenced by the composition of the reducing gas, its pressure, and its temperature, the small differences in the α^*_{hkl} values for the samples from (*3*) and (*5*) in Table 4 result. The observed $\bar{L}_{hkl}$ values also give an indication of the shape of the particles. From (*3*) and (*5*), the $\bar{L}_{200}$, $\bar{L}_{110}$, and $\bar{L}_{222}$ values indicate a shape which may be described as a combination of a cube and an octahedron.

TABLE 4

α^*_{hkl} Values for M-2.2Al Reduced at 400°C, Additionally Reduced in H_2 at 800°C (*3*), and for M-1.3Al Reduced at 500°C, Additionally Heated in an Inert Atmosphere at 800 and 900°C (*5*)

Sample	Temperature (°C)	*hkl*		
		200	110	222
M-2.2Al	400	0.19	0.12	0.26
	800	0.19	0.10	
M-1.3Al	500	0.18	0.13	0.29
	800	0.14	0.10	0.27
	900	0.14	0.09	

3. *Stability of Paracrystalline Iron, "α-Fe"*

By reduction of magnetite with additional statistically distributed cations as Al, Sc, Cr, etc. in H_2 at temperatures of 350–500°C, endotactic groups form which are less mobile than the Fe atoms. These individual groups remain therefore for the most part statistically distributed in the growing "α-Fe." These groups produce an unevenness in the lattice planes which above a certain value of N_{max} prevents the further orderly growth of the "α-Fe" particle.

Thermal treatments of paracrystalline iron, "α-Fe," at temperatures higher than 500°C are shown in Fig. 7. Separate parts of the M-1.3Al sample, which was reduced at 500°C, were heated in a vacuum for 20 hr at 800, 900, and 950°C, respectively

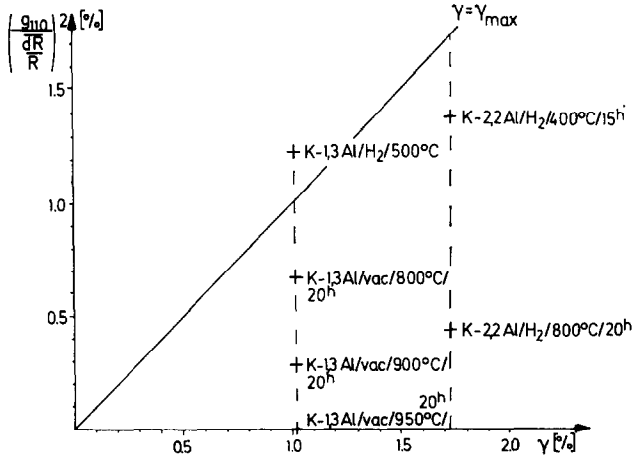

FIG. 7. M-1.3Al reduced at 500°C, then heated in a vacuum at 800, 900, and 950°C, and M-2.2Al reduced at 400°C, then heated in H_2 at 800°C, plotted in the diagram as percentage of endotactic groups $[g/(\overline{dR}/R)]^2 = \gamma$ against percentage of Al_2FeO_4 groups $[\gamma_{max}]$.

(*5*). The g_{hkl} values decreased at higher temperatures and become zero at 950°C. Below 950°C no phase was observed other than paracrystalline iron, "α-Fe." After heating at 950°C, α-Fe and hercynite ($FeAl_2O_4$) were observed. This was interpreted by Fagherazzi *et al.* (*5*) as a segregation of the endotactic groups and formation of hercynite during the transition of the bcc iron to fcc iron (γ-Fe).

Separate parts of the M-2.2Al sample, which was reduced at 400°C (*3*), were treated in a H_2 stream for 20 hr at 800 and 950°C. The g_{hkl} value was lowered at 800°C (see Fig. 7) and was zero at 950°C. X-ray diffraction of the latter one shows α-Fe and β-Al_2O_3. This result can be interpreted as being similar to case of the M-1.3Al sample: At the transition of the bcc iron to the fcc iron (γ-Fe), endotactic groups segregate and are reduced in the H_2 stream to form β-Al_2O_3.

As seen in Fig. 7, the g values decrease at increasing temperatures under otherwise equal conditions. This can be explained through Eq. (3) by the fact that the number of endotactic groups is smaller. The following possibilities would explain the decrease of the number of endotactic groups: (i) The endotactic groups form clusters inside the "α-Fe" or/and (ii) the endotactic groups partially emigrate to the surface of the "α-Fe." Experiments are planned to determine the dominant process.

V. CONCLUSIONS

The lattices of iron catalysts promoted with oxides of trivalent cations of metals such as Al, Sc, Cr, etc. ("α-Fe") are paracrystalline. The crystal chemical properties of the "α-Fe," such as lattice constant, Curie point, and density of states of the electrons, are the same as for pure α-Fe. The paracrystallinity is caused by endotactic groups "X_2FeO_4," with X = Al, Sc, Cr, etc., lying statistically distributed in the "α-Fe." The "α-Fe" is formed by the reduction process at temperatures below 600°C directly from the spinel. At temperatures of 350–500°C the "X_2FeO_4" groups are mostly individual ones. The low mobility of the endotactic groups in this temperature range is responsible for the stability of the small "α-Fe" particles. This small size of about 300 Å for the "α-Fe" particles is determined by the paracrystallinity (g_{hkl}) and the α^*_{hkl} values [Eq. (4)].

Thermal treatments of "α-Fe" at higher temperatures result in decreased paracrystallinity and increased particle size. After heating for several hours at 950°C, no paracrystallinity is observed. This is explained by a segregation process of the endotactic groups and the formation of a new crystalline phase during transition of the paracrystalline iron to γ-Fe. Besides α-Fe, $FeAl_2O_4$ (hercynite) was found under vacuum conditions and β-Al_2O_3 was found under H_2 conditions.

REFERENCES

1. Frankenburg, W. G., *in* "Catalysis" (P. H. Emmett, Ed.), Vol. 3. Reinhold, New York, 1955.
2. Nielsen, A. "An Investigation on Promoted Iron Catalysts for the Synthesis of Ammonia," 2nd ed., Jul. Gjellerups, Copenhagen, 1956.
3. Hosemann, R., Preisinger, A., and Vogel, W., *Ber. Bunsenges. Phys. Chem.* **70**, 797 (1966).
4. Pernicone, N., Fagherazzi, G., Galante, F., Garbassi, F., Lazzerin, F., and Mattera, A., *in* "Proceedings. 5th International Congress on Catalysis, Amsterdam, 1972." North-Holland, Amsterdam, 1972.
5. Fagherazzi, G., Galante, F., Garbassi, F., and Pernicone, N., *J. Catal.* **26**, 344 (1972).
6. Topsøe, H., Dumesic, J. A., and Boudart, M., *J. Catal.* **28**, 447 (1973).
7. Buhl, R., and Preisinger, A., *Surface Sci.* **47**, 344 (1975).
8. Hofmann, E. G., and Jagodzinski, H., *Z. Metallk.* **46**, 601 (1955).
9. Hosemann, R., and Bagchi, S. N., "Direct Analysis of Diffraction by Matter." North-Holland, Amsterdam, 1962.
10. Warren, B. E., *Acta Crystallogr.* **8**, 483 (1955).
11. Vogel, W., Haase, J., and Hosemann, R., *Z. Naturforsch.* **29a**, 1152 (1974).

12. Turnock, A. C., and Eugster, H. P., *J. Petrol.* **3**, 533 (1962).
13. Akimov, V. M., *Izv. Akad. Naut. SSSR Ser. Khim* **12**, 2208 (1963).
14. Walson, I. E., and Thomassen, L., *Trans. Amer. Soc. Metals* **22**, 769 (1934).
15. Garbassi, F., Fagherazzi, G., and Calcaterra, M., *J. Catal.* **26**, 338 (1972).
16. Hosemann, R., *Endeavour* **32**, 99 (1973).
17. Greenwood, N. N., and Gibb, T. C., "Mössbauer Spectroscopy." Chapman and Hall, London, 1971.
18. Taylor, A., and Jones, R. M., *Int. J. Phys. Chem. Solids* **6**, 16 (1958).
19. Graham, M. J., Channing, D. A., Swallow, G. A., and Jones, R. D., *J. Mater. Sci.* **10**, 1175 (1975).